Enhancing precision and reliability of tri-axial load cells for mooring load measurements

M. Ponomarev[1], L. Johanning[2] and D.N. Parish[3]

University of Exeter,
Engineering, Mathematics and Physical Sciences, Renewable energy group
Cornwall Campus, Treliever Road, Penryn, TR10 9EZ, UK

[1] E-mail: M.Ponomarev@exeter.ac.uk

[2] E-mail: L.Johanning@exeter.ac.uk

[3] E-mail: D.N.Parish@exeter.ac.uk

Abstract

A mooring test facility (South West Mooring Test Facility – SWMTF) has been developed of the coast of Cornwall by PRIMaRE and CORES members at the University of Exeter. It has unique features so it can obtain very detailed data in actual sea conditions to show how moored structures respond to changes in wind, wave, current and tide. Using this information, developers, or associated companies, will be able to model and test mooring designs and components for marine energy devices as they convert wave movement into energy.

The SWMTF buoy has a simple, circular design, with specialised sensors and other instruments built into its structure, enabling it to record data to a high degree of accuracy and allow real time data communication to shore. The novel sensing package allows collecting detailed load and response data in actual sea conditions.

One of the key instrument within this package are the tri-axial load cells. Within this paper the calibration of the tri-axis load cell is described and how this measurement technique can contribute to survivability of floating marine energy devices.

Keywords: WEC mooring configurations, Tri-axis load cell, tension measurement, calibration

1. Introduction

The announcement of large-scale marine energy projects like the planned 1.2 GW installation of wave and tidal devices in the Pentland Firth [1] mark the emergence from the prototype and demonstration stage to commercial deployment of marine energy converters (MECs). The viability and success of these projects is strongly dependent on the reliability of devices as this determines the amount of generated electricity and the cost for operation and maintenance.

In order to inform and support the MRE industry in the establishment of component reliability data, the PRIMaRE group at the University of Exeter developed a purpose built mooring test facility (SWMTF) and a Dynamic Marine Component Test rig (DMaC). The combine application will allow i) component tests under service simulated conditions and ii) to conduct accelerated component testing. The results from the component tests under service simulated conditions will provide load characteristics that can be used to inform the accelerated testing. The application of such component reliability testing can reveal design weaknesses prior to deployment and support development of specific components. Subsequently design performance, expected lifetime and subsequently support (cost-) optimisation of marine renewable energy (MRE) devices can be evaluated.

This paper is focusing on the design, calibration and analysis methodology of the tri-axis load cells, a key instrument to measure the mooring leg tension in its x-, y- and z-component. Present load cell designs do not contain an absolute internal reference for measuring forces but they can achieve certain accuracy only through calibration relative to some known reference. Calibration procedure is more difficult for tri-axial load cells due to almost unavoidable cross-coupling between sensors for different axes (components). In addition, due to increased complexity of the multi-component systems there are more chances to have the tri-axial load cells produced with some manufacture defects. These defects could generate sets of outliers (gross errors) in the measurements, which need to be identified.

A method is described for processing the data generated by tri-axial load cells which allow to identify and correct gross errors in sets of measurements. These are then used to identify which vector sensor component has outliers. Within the study a model has been developed for cross-validation of a three-component system. In addition, for extreme case of single component failure it is proposed to use prior calibration equation. This allows obtaining credible three component force measurements even if one component has significant outliners.

2. Uncertainties in mooring design

Resonance modes of floating wave energy converters (WECs) can be assumed to be close to excitation modes as a result of the body size and its application to produce power from first order waves. In the case for moored WEC devices additional complexity is given through the analysis requirement of the coupled system. The implications this can have to the design of WEC devices are manifold and hence a good understanding of the dynamic response of the floating system is required. This is because the reliability, design performance, expected lifetime and subsequently cost optimisation of WEC devices are directly linked to the prediction of the load and response characteristics.

Consequently, in order to identify the correct response of a coupled moored WEC device, the equation of motion has not only to consider the load and response behaviour of the structure, but in addition the influence of the mooring system and the power-take-off (PTO) system. Hence the equation of motion for a moored WEC device in its six degree of freedom (DOF) ξ_j must be expressed in the form

$$\sum_{j=1}^{6}\left[-\omega_i^2\left(M_{ij}+A_{ij}+M_{ij}^{E}\right)+i\omega_i\left(B_{ij}+B_{ij}^{E}+B_{ij}^{PTO}\right)+\left(C_{ij}+K_{ij}\right)\right]^{-1} F_i=\xi_j \quad (1)$$

with i = 1,…,6 being the complex amplitudes of the exciting forces F_i at the related excitation frequencies ω_i and j = 1, ..., 6 the response modes.

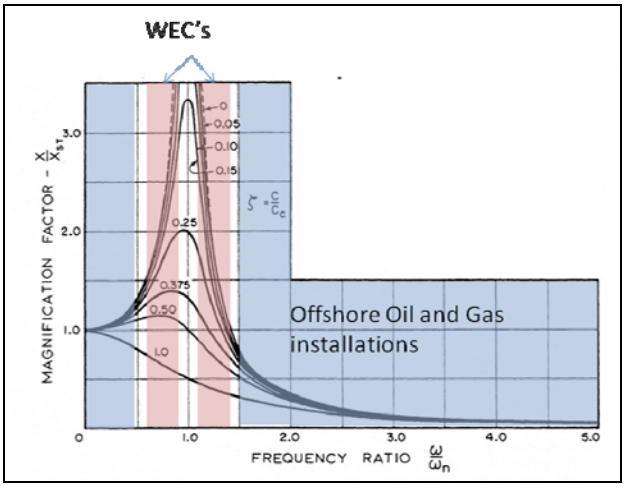

Figure 1: Illustration of response variation between WEC devices and offshore oil and gas installations

As a result the degrees of motions must be calculated from the directional excitation forces and the corresponding mass matrix of the body M_{ij}, the added mass matrix A_{ij}, the damping matrixes B_{ij} and B_{Eij} and the stiffness matrixes C_{ij} and K_{ij}. The damping matrix B_{ij} and the stiffness matrix C_{ij} are directly related to the floating structure, and represent the radiation damping and viscous damping (including vortex shedding) and the hydrostatic and gravitational stiffness respectively. The external mass matrix M_{Eij}, damping matrix B_{Eij} and stiffness matrix K_{ij} describes the mass (mass and added mass), damping source and stiffness properties from the mooring system, and B_{PTOij} is the power take-off damping.

Often for the response and load analysis of typical oil and gas offshore structures a 'quasi'-static approach can be applied since such floating devices are designed well of the resonance mode (figure 1). However, for mooring applications where the station keeping of a structure cannot be considered to be in a 'static' mooring regime, non-linear mooring behaviour contributes importantly to the tension characteristics of the moor. As discussed by Mavrakos et.al. [2] this became a great concern for deep sea mooring installations, where the elastic stiffness of the cable becomes the principal parameter affecting the mooring line's dynamic response and, hence, it's non-linear behaviour. Non-linear mooring behaviour has been addressed in several publications (Papazoglou et.al. [3], Webster [4], Raajimakers and Battjes [5], Aranha and Pinto [6], Johanning et.al. [7]).

Whilst fully dynamic numerical simulation models are improving steadily, capable of implementing non-linear behaviours, these models often rely on input parameters such as stiffness and damping characteristics. One of the important factors governing the non-linear response is the role of viscous energy dissipation, when either the amplitude of displacement or the frequency of the top-end motion (induced by the attached device) increases. Considering a coupled moored system the contribution of non-linear response not only influences importantly the tension characteristics of the lines, but also the mooring reactance and resistance in form of stiffness and damping respectively and, hence, the motion characteristics of the floating structure and component reliability.

As a consequence damping characteristics needs to be identified to establish the response behaviour of a moored WEC to a high accuracy from numerical dynamic models. In-situ tests in realistic situations can aid to obtain such data that can be applied to calibrate and /or validate these simulation models.

3 South Western Mooring test facility

The South Western Mooring Test Facility (SWMTF) is a unique mooring load and response test facility, at large scale in real sea condition, and has been recently installed at Falmouth Bay, Cornwall, UK (Figure 2). The SWMTF facilities will allow measuring loads that

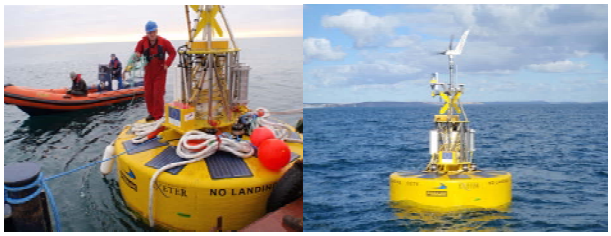

Figure 2: South Western Mooring Test Facility (SWMTF) buoy during launch and operation

are experienced in the field through prototype testing, which information can be subsequently replicated to perform accelerated component testing under simulated in-service field conditions.

It is instrumented to gather data relating to the response of the buoy and the mooring line tensions due to external loads [8]. The influences of wave action, tidal currents, wind blown surface currents and wind are being measured by the following instrumentation:

- On the buoy:
  - Six degree motion measurement system
  - Differential Global Positioning System (DGPS)
  - Structural stress measurements
  - Directional wind data on buoy
- Mooring system:
  - Tri-axis top-end load cell
  - In-line load cells
  - Anchor point load cells
  - Mid-line load cells
- Environmental condition monitoring:
  - Multiple acoustic Doppler systems for waves/current (ADCPs)
  - Onshore weather station
  - Water quality measurements

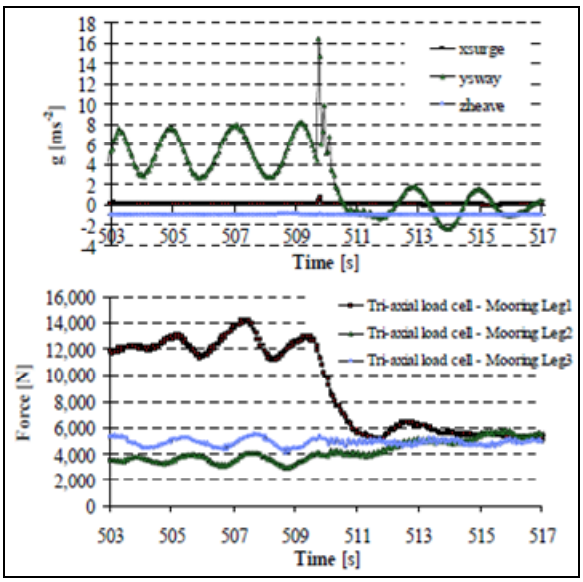

Figure 3: SWMTF response and mooring tension data

Processing of the data (figure 3) will give a thorough understanding of the loads imposed on the system, which information can be used for calibration and validation of six-degree of freedom model, such as compiled within the FP7-CORES project by the Wave Energy Centre (WavEC). In addition the results can be used to compare and inform industrial offshore analysis finite element package, such as Flexcom [9] or OrcaFlex [10], and inform the reliability analysis of specific components as discussed by Thies and Johanning [11].

4. Tri-axis load cell

4.1 Design of Tri-axis load cell

A key requirement of the buoy's instrumentation is the measurement of the top-end mooring tension in its x-, y- and z-components which provides for a resultant force vector. Since no suitable on-the-shelf load cell could be identified for this task, a tri-axis, tension load cell was designed in collaboration between PRIMaRE engineers and Elite Transducers Ltd.

The design incorporates a two-degree of freedom swivel between the strain gauged element and the mooring take off point, thereby ensuring that the strain gauge responses properly reflect the force vectors applied (figure 4).

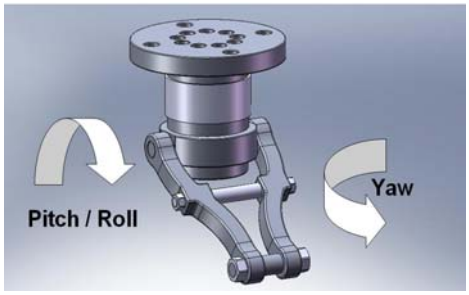

Figure 4: SWMTF Tri-axis Load Cell Assembly

Dynamic simulation analysis of the buoy with the proposed three limbed mooring arrangement was conducted for the worst case wave, wind and current loading. The result predicted a peak loading at the top end attachment for a single limb of 69KN. In common with all other structural components in the buoy and mooring system, a factor of safety, three, was applied to the design ensuring a high degree of structural reliability.

4.2 Calibration methodology

Calibration of each individual axis (x, y, z) was performed by Elite Tranducers Ltd according to their normal single axis load cell practice.

However, it was necessary to identify the mechanical cross talk between axes. For this purpose an in-depth calibration of the load cells was required to obtain calibration data for a sufficient number of compound angles, which defines the operational hemisphere of the tri-axis load cells. To obtain the calibration data, a dedicated fixture was designed and constructed at the University of Exeter. The fixture locates within a MTS tensile/compressive test machine (figure 5) which was programmed to step up through 20 tensile load values, to a maximum of 50 kN at each compound angle setting. The compound angles provided by the fixture

Figure 5: Dedicated Calibration Fixture Located within MTS Tensile Test Machine

result from π/16 radian increments in both azimuth and zenith (drop angle of mooring limb).

Adjustment of the zenith angle was achieved by means of the swinging frame and a location dowel pin. The pivot axis of the swinging frame was designed to be coaxial to the pitch/roll swivel axis of the tri-axis unit, ensuring that the location dowel takes no real loading during the test. The adjustment of the azimuth angle is provided by the choice of mounting holes provided by the swinging base plate and a changeover swinging base plate.

For a given load applied, the true force vector can be described as a point on the surface of a hemisphere. The set of these points forms a regular grid over the surface of the hemisphere (Figure 6). Deviation from these regular grid points on the hemisphere represents tri-axis output error which requires correction.

4.3 Analysis Methodology

The first stage of data analysis has been to check out voltage readings obtained during experimental calibration procedure. A set of measured preloaded three-dimensional resulting forces vector $\vec{F} = (F_x;F_y;F_z)$ has been assessed against corresponding three-dimensional resulting voltage vector $\vec{V} = (V_x;V_y;V_z)$. These have been taken from averages calibration voltage samples, measured during the calibration proceedings at the MTS rig.

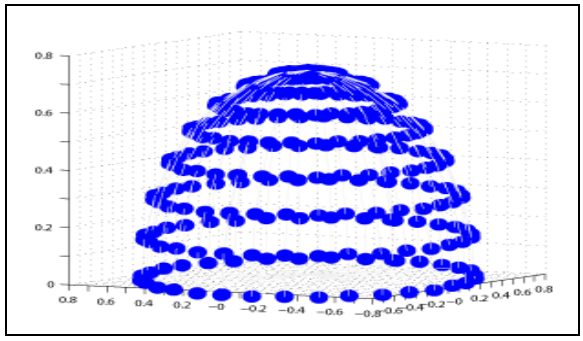

Figure 6: 5tonne calibration data result (uncorrected)

The second step was to take voltage samples for load cell LC4, load cell LC5 and load cell LC6, which correspond to a numbers of different forces. The outcome of these voltage samples over the range of forces provides a semi-sphere calibration map (figure 6). Every constant point load was sampled over 5 second during which period 50 voltage readings were taken. To avoid transient effects, averaging has been undertaken over 40 voltage readings, ignoring the 5 first and last readings.

The next step for the analysis was to calculate the relationship between absolute voltage $V = \sqrt{V_x^2 + V_y^2 + V_z^2}$ and absolute force $F = \sqrt{F_x^2 + F_y^2 + F_z^2}$. The outcome of this analysis should result in a linear regression line in form:

$$V = kF + V_0 \qquad (1)$$

Figure 7 shows scatter plots of absolute voltages (y-axis) as functions of absolute forces (x-axis). The absolute forces were predefined as a discrete set of 20 loads ranging from 1kN to 50kN. The solid line represents the linear regression in figure 7.

This preliminary screening detected problems for LC4

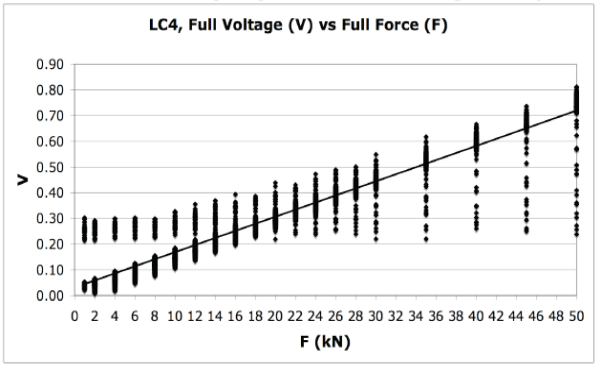

Figure 7: calibration reading for tri-axis load cell LC4

(figure 7) and LC5. It has been noticed that both plots contain a majority of data points in the vicinity of the regression line, however there are considerable deviations too. This observation was only made for LC4 and LC5, whilst for LC6 no outstanding deviations could be detected.

Within the next step it needed to be identified which individual vectors in the x-, y- and z-component contributed to the observation of deviations. No contamination was found in both the x- and y-component for LC4, LC5 and LC6, applying a 95 percent confidence interval and ignoring close to zero readings. From the analysis of the individual components it was identified that only the z-component contributes to the observation of considerable deviations.

Figures 8a-c outlines the results of the deviations for LC4, LC5 and LC6 in the z-component. Distinctive branches of deviations (outliers) can be observed for

LC4 and LC5 (Figure 8a,b). However, this observation was not made for LC6 (Figure 8c), which agrees with the findings in the resulting vector analysis. The contamination in the z-axis for LC4 was established to be about 10%, whilst for LC5 in the order of 2%.

The appearance of these outliers in a localised area allowed removing these with high confidence from the data set.

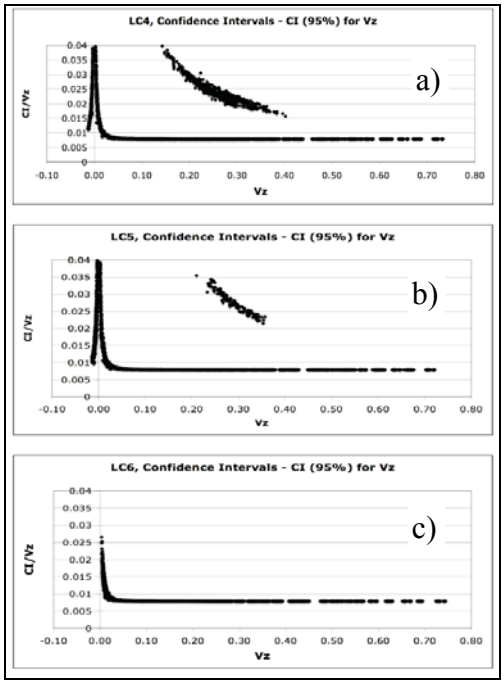

Figure 8a-c: Scatter plots for the 95 percent confidence intervals for z-component, a) LC4, b) LC5, c)LC6

4.3.1 Regression based analysis

The regression based method [12] can be used to interpret the load in terms of a polynomial equation

$$V_i = \sum_{j=x}^{z} a_{ij} F_j + V_{i0}, \qquad (2)$$

where sensitivity coefficients a_{ij} are calculated from the least square fit to the data set including force radial components F_x , F_y and F_z. In addition the possible shift has been included in equation (2) through V_{i0} = (V_{x0} , V_{y0}, V_{z0}). This could be different for each load cell. The sensitivity coefficients a_{ij} constitute a response matrix ||A|| that needs to be identified. For each load cell a response matrix was calculated.

Below the response matrixes ||A|| are outlined for the load cell LC4 without the removal of outliers. The full set of calibration data (FSD) response matrix was found to be

$$A_{LC4\_FSD} = \begin{vmatrix} 14.9416 & 0.0292 & 0.1908 \\ -0.4369 & 15.0632 & 0.0580 \\ 0.5156 & 0.6619 & 13.1017 \end{vmatrix}$$

with $\vec{V}_{0\_LC4\_FSD} = (-30.3739\ ; -20.3383\ ; 26.7828)mV/V$, mean absolute deviation (MAD) of (4.2; 4.2; 34.7)mV/V and standard deviation (STD) of (5.4; 6.2; 62.2)mV/V.

In contrast the response matrixes ||A|| for the load cell LC4, removing the outliers, the response matrix was found to be

$$A_{LC4} = \begin{vmatrix} 14.9374 & 0.0154 & 0.1915 \\ -0.4328 & 15.1311 & 0.0657 \\ 0.4160 & 0.1385 & 14.7828 \end{vmatrix}$$

with $\vec{V}_{0\_LC4\_FSD} = (-31.0530\ ; -20.2394\ ; -3.0337)mV/V$, mean absolute deviation (MAD) of (3.9; 4.1; 3.0)mV/V and standard deviation (STD) of (5.2; 6.1; 3.8)mV/V.

The larger numbers on main diagonals of calculated sensitivity matrixes define the larger contribution to any particular component of voltage response (V_x,V_y,V_z) from the corresponding force components (F_x, F_y, F_z). Any off-main diagonal numbers define cross-talks forces.

4.3.2 Substitution Model

For data analysis purpose a general substitution model was introduced. This model allows the establishment of matrix of precision zones for each three-dimensional sensor component from. From these matrixes it can be establish which of the components contribute to the largest error in three-dimensional precision calibration space. Once the precision calibration matrix is established it could be applied in conjunction with the replacement model to identify the vector component with the highest local error. The replacement model needs to be designed to reflect realistically on the physical implication. This procedure helps to increase the measurement precision, both for the particular vector sensor component and for full three-dimensional force reading.

Applying this substitution model to the calibration of the load cells L4 and LC5, with significant outliers in the z-component, these can be detected from

$$\left| F_z^{out} - F_z^{med} \right| > \Delta_{Fz}^{\max}, \qquad (3)$$

where F_z^{out} are the force outliers, $\Delta_{Fz}^{\max}$ the maximal absolute deviation from the regression line F_z^{med} . By applying this model individual outlier are replaced with

$$F_z^{med} = \sqrt{\frac{1}{k^2}(V - V_0)^2 - F_x^2 - F_y^2} \pm \Delta\ , \qquad (4)$$

where k and $V_0 = \sqrt{V_{0x}^2 + V_{0y}^2 + V_{0z}^2}$ could be obtained from regression. The force F_x and F_y represent here calibrated measured forces. Here Δ is proportional to the standard deviation and having the direction of absolute deviation. This regression based replacement

model allow to detect the outliers in real-time and replace them with those of real physical model.

Once the model has been established for a specific case, a cross check should be performed. This has been done for all load cells (LC4, LC5, LC6) in the resulting vector component using a representation of relative prediction error (RPE).

$$RPE = \sqrt{\frac{(\dot{F}^p - \dot{F}^n)^2}{(\dot{F}^n)^2}} * 100\% \quad , \qquad (5)$$

where the predicted force $\dot{F}^p = (F_x^p; F_y^p; F_z^p)$ was examined against the known force $\dot{F}^n = (F_x^n; F_y^n; F_z^n)$.

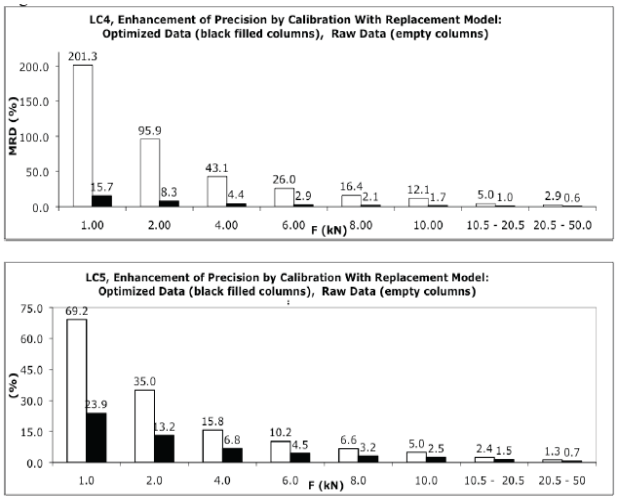

Figure 9a,b: Error calculation for corrected and non-corrected calibration tests

Fig. 9a,b compares the none-corrected (white) and corrected (black) results of the relative prediction error (RPE) for LC4 and LC5. The analysis was conducted for loads between 1 and 10kN with at a 2kN step, and for a load range between 10.5-20.5kN and 20.5-50kN. It can be clearly seen that by applying the substitution model allowing for correction of outliers the RPE is reducing significantly at lower loads.

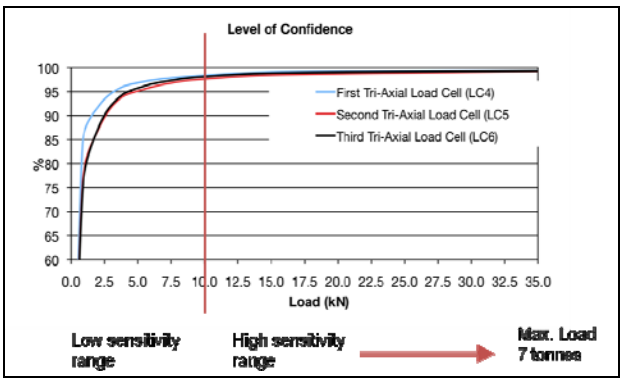

Figure 10: Level of confidence for load cells LC4, LC5 and LC6

Fig.10 represents the level of confidence of force readings for the load cell LC4, LC5 and LC6. The confidence level presented in figure 10 includes the correction of outliers. It can be seen that at the low sensitivity range (0 – 10kN) the percentage confidence is increasing reaching 95% at approximate 5kN. At the high sensitivity range (10 – 35kN) the percentage confidence is approaching 100%. The load cells where designed for a measuring range between 5kN and 50kN to allow for withstanding extreme loads.

5 Conclusions

A design, calibration and analysis methodology for tri-axis load cells, a key instrument to measure the mooring leg tension in its x-, y- and z-component to measure dynamic tension characteristics, has been presented. A method is described for processing the data that allows correcting gross errors in sets of measurements. It is shown that precision is not a single number for points throughout the whole load range but depends on the value of the load. It is demonstrated that the described analysis model will enhance precision of the force output up to 10 times for loads range 1-10kN. The result gives confidence in the methodology and is applied in the data analysis for the SWMTF measurements. It is explained how the measurement from the SWMTF can be used to inform numerical simulation models and subsequently support the reliability and cost optimisation of MRE devices.

References

[1]The Crown estate (2010) World's first wave and tidal energy leasing round, Press Release, 16 March 2010. http://www.thecrownestate.co.uk

[2]S. A. Mavrakos, V. J. Papazoglou, M. S. Triantafyllou & J. Hatjigeorgiou (1996) Deep Water Mooring Dynamics, Marine Structures 9, pp 181-209

[3]Papazoglou, V.J., Mavrakos, S.A. and Triantafyllou, M.S. (1990) Nonlinear cable response and model testing in water, Journal of Sound and Vibration, 140(1), pp 103-115

[4]Webster, W.C. (1995), Mooring-induced damping, Ocean Engineering, Vol. 22 (6), pp. 571-591

[5]Raaijmakers, R.M. and Battjes, J.A. (1997) An experimental verification of Huse's model on the calculation of mooring line damping, Proceeding of the 8th BOSS conference, Vol. 2, pp 439-452.

[6]Aranha, J.A.P. and Pinto, M.O. (2001) Dynamic tension in risers and mooring lines: an algebraic approximation for harmonic excitation, Applied Ocean Research, Vol. 23, pp 63-81

[7] Johanning, L., Smith, G.H. and Wolfram, J., (2007); Measurements of static and dynamic mooring line damping and their importance for floating WEC devices, Ocean Engineering, Vol. 34(14-15), p. 1918-1934

[8]Johanning L., Spargo A. and Parish D.N. (2008) Large scale mooring test facility – A technical note, 2nd Int. conference on Ocean Energy (ICOE 2008), 15 - 17 October 2008, Brest, France

[9]MCS Kenny (2009); Flexcom, Galway Technology Park, Parkmore, Galway, Ireland, galway@mcs.com

[10] Orcina (2007) OrcaFlex User Manual, Version 9.1a; Orcina Ltd., Ulverston, Cumbria, LA12 7AJ, UK, www.orcina.com

[11] Thies P.R. and Johanning L. (2010) Development of a marine component testing facility for marine energy converters, 3rd Int. conference on Ocean Energy (ICOE 2010), 06 - 08 October 2010, Bilbao, Spain

[12] Maindonald J.H., Statistical Computation, John Wiley & Sons Inc., 1984

Acknowledgements

The authors would like to acknowledge the support of the South West Regional Development Agency, in their support of the development of the mooring test facility, and would also like to thank Orcina Ltd for providing us with their simulation software OrcaFlex and their subsequent support. This project is partially funded by the European Commission (FP7-CORES) under grant agreement n° 213633.